Refiner Optimization and Control Part I: Fiber residence time and major dynamic fluctuations in TMP refining processes

Anders Karlström and Jan Hill

KEYWORDS: Refining control, energy efficiency, fiber distribution, pulp consistency, temperature profile

SUMMARY: The focus is dynamic considerations in a mill-wide perspective and it is shown that the mill economy is closely linked to how the TMP and the power plant are optimized. Special attention is given to stability issues in the refining processes, as the stabilization of the fiber pad inside the refining zone is complex and will be affected by a number of disturbances not very well specified in traditional stationary models. Describing the dynamics in such nonlinear processes is difficult and tedious and requires significant knowledge about where in the operating window to run the refiners.

In this paper we will show the dynamics in the internal states, temperature profiles and the plate gap sensors responses and how they correspond to the refiner motor load. It is also shown that disturbances in production affect the plate gap sensors and the temperature profiles in the same direction, while deliberate changes in the plate gap result in a dynamic situation where the motor load and temperature profile change in opposite directions.

There is a special focus on the residence time variations in different parts of the refining zone. It is shown that the total residence time and the ratio between the residence time before and after the maximum temperature will be important when formulating specifications for energy efficient refining.

As an example of how the refining process affects the mill economy, the start-up procedures for two different types of refiners will be penetrated. It is shown that the start-ups are most often associated with an over shoot in the motor load, which is easy to overcome.

ADDRESSES OF THE AUTHORS:
Anders Karlström (anderska@chalmers.se**),** Chalmers University of Technology, Göteborg, Sweden
Jan Hill (jan.hill@qtab.se), QualTech AB, Sweden
Corresponding author: Anders Karlström

Most papers dealing with refiner optimization and control confine themselves to discussing the topic either with the perspective of an individual refiner or an individual TMP production line. Some examples of this approach can be found in Hill et al. (1979), Johansson et al. (1980), Dahlqvist and Ferrari (1981), Oksum (1983), Honkasalo et al. (1989), Hill et al. (1993), Berg (2005), Eriksson (2005), Eriksson (2009) and Karlström and Isaksson (2009).

It is rather seldom that the consequences of the refiner operation on the total mill energy balance are addressed. This matter is either addressed in the design of a mill or when altering the process configurations in an existing mill. On this occasion the procedure is usually to calculate three operating scenarios: maximum, average and minimum demand cases. In this way the operating windows of the different sub-processes of the mill are established. These calculations are in the vast majority of cases carried out from a static point of view, while handling dynamics is directed to the design of the different sub-processes.

Energy balances and energy optimization of existing mills are usually studied with a similar static approach but with other methodology than during the design phase. Some examples of this approach can be found in Noël (1995), Shaareman et al. (2000), Lafourcade et al. (2003), Axelsson and Berntsson (2005) and Rouhonen and Ahtila (2009). Thus, there are few studies in which the actual mill dynamics ranging from fractions of a second up to months are penetrated.

The electrical energy used in an integrated mill producing publication papers based on TMP is dominated by the electrical energy use of the refiners – see e.g. Jönsson (2011). Thus the dynamics of the refiners has a major influence on the electrical energy dynamics of the mill.

There are four rather clear classes of cases that ought to be considered when studying the impact of the refiners on the mill energy dynamics: 1) Refiner not in operation with or without idling electrical motor; 2) Start-up of refiner(s), either the motor(s) alone or the start of production – the latter case being the most interesting in this perspective; 3) Refiners in continuous operation at normal process targets; 4) Instantaneous stop of one or more refiners, which can happen as a planned or as an unplanned action.

This paper presents a theoretical model taking consideration to the dynamics of the electrical energy in the context of steam demand of the mill operation. Further, continuous operation and start-ups of pulp production are given as examples. Furthermore, it is rare to find refiner control papers that address the impact of the control on the conditions in the refining zone and thus pulp properties produced in the short term, see Karlström et al. (2008). It is usually assumed that operating the refiner with unchanged and properly selected set points will in the short perspective imply stable operating conditions and uniform pulp quality. Unfortunately this is not the case, as most of the disturbances are related to the chip or pulp feed – see e.g. Hill et al. (1993) and Ferritsius et al. (2014). In addition, the slow dynamics of the control loops of the refiner system will deteriorate the stability in the refiner gap - see Appendix C. This statement is also strengthened by earlier published fundamental models by Karlström and Eriksson (2014a,b,c,d), which in this paper are used to evaluate the

stability in the refining zone based on estimated residence time.

This paper is the first in a series of five consecutive papers. The idea is to broaden the discussion of how to use more sophisticated refining zone measurements in future control concepts to reach maximized process uptime and the full refining optimization potential both with respect to pulp property development and as a major player in the mill-wide energy optimization perspective. This series is ended by a comprehensive systems approach on energy dynamics in the mill-wide perspective and its implications for both mill operations and mill economy and how to further improve future control concepts.

Fundamentals

TMP in a broader perspective: The easiest way to describe the mill situation is to start with the product specification, i.e. which paper quality to produce. This sets the boundaries for the mill model, as each paper quality has its own operating window and process limitations. The operating windows for newsprint paper production can be interpreted as acceptable regions for operating the thermo-mechanical pulp mill (TMP), the power plant (PP) and a number of paper machines (PM), see *Fig. 1*.

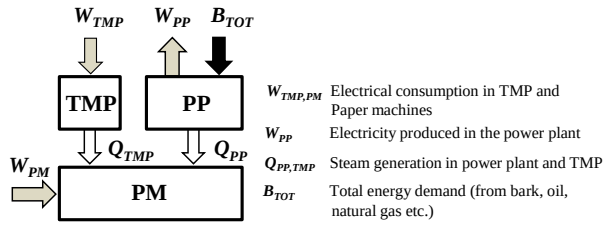

Fig. 1: Schematic overview of a newsprint mill from an energy perspective.

The boundaries for the operating windows can be seen as the natural process limitations, which are indeed difficult to pre-specify.

All plants have to be conscientious about the intake of fresh water and the release of process water to further effluent treatment. This is a rather substantial heat sink[1], in particular in mills with high fresh water consumption per ton of paper produced. Often a plant for recycled fiber supply exists as well, but this is not included as it stands for a minor energy sink[2] of the total mill economy. These are in this consideration treated as static heat sinks. Hence, it is essential to optimize the main consumers from an overall energy consumption perspective where the largest electrical consumer to focus on is the TMP mill.

Starting with the schematic overview of a newsprint mill, it is straightforward to formulate the basic ideas. Knowing the steam production in the power plant[3], Q_{PP}, and the surplus of the TMP mill, Q_{TMP}, the steam required in the paper machines is easy to derive[4] as

$$Q_{PM} = Q_{TMP} + Q_{PP}$$

The total electrical consumption in the mill, W_{TOT} , can in a similar way be formulated as

$$W_{TOT} = W_{TMP} + W_{PM} - W_{PP}$$

In a similar way the energy demand from bark, oil, natural gas et cetera, here represented by the variable B_{TOT} in *Fig. 1*, can be formulated.

By introducing the boiler efficiency, η_P, the energy demand, B_{TOT}, can be described as the sum of the energy in the produced steam and electricity divided by the boiler efficiency i.e.

$$B_{TOT} = (Q_{PP} + W_{PP})/\eta_P$$

The electricity, $W_{PP,}$ is produced in a generator and can be estimated as a linear function of the amount of produced steam, Q_{PP},

$$W_{PP} = \alpha Q_{PP} + C_\alpha$$

where α is the proportionality constant between steam and electricity production and C_α is the no-load steam consumption of the generator.

The TMP mill stands for about 70% of the electricity consumption in the mill and varies considerably over time depending on the refiner runnability etc. As the electricity consumption in the TMP mill also affects the steam balance directly, as the refiners are the main producers of steam to the plant, it is natural to study the TMP mill[5], where even small deviations from production set points will affect the energy balance as well as the pulp properties.

Dynamic considerations are best described by differentiating the electrical consumption in the mill, W_{TOT} , with respect to time and the vector u containing the elements P, representing the production rate of pulp in the refiners, h, the hydraulic pressure applied to refiner discs, and D, the dilution water feed rate.

$$W_{TOT} = f(u) \quad ; \quad B_{TOT} = g(u) \quad ; \quad u = [P, h, D]^T$$

$$\frac{\partial}{\partial t}(W_{TOT}) = \frac{\partial}{\partial u}(W_{TOT}) \cdot \frac{\partial}{\partial t}(u) \quad ; \quad \frac{\partial}{\partial t}(B_{TOT}) = \frac{\partial}{\partial u}(B_{TOT}) \cdot \frac{\partial}{\partial t}(u)$$

[1] In an integrated mill, this energy demand is approximately proportional to the fresh water consumption per tonne of paper produced. This is a heat sink with slow dynamics compared to the electrical energy demand and steam demand, respectively. Thus this is regarded as a static heat sink and excluded from the following discussion. The energy demand per tonne of fresh water is impacted by the degree of heat exchange of water – steam to the air and the water to the effluent treatment, respectively.

[2] Approximately 350 kWh/t.

[3] Note that the variable *Q* is in fact the rate of heat. In the literature these variables are referred to as steam generation, which sometimes can be a misleading word, especially when these variables are combined in an overall energy balance where also the electrical consumption, *W*, is included.

[4] There are some additional steam usages in the heating of water and fibers in the process. As earlier stated, these heat sinks can be regarded as rather static, but they will naturally increase B_{TOT} in reality.

[5] In many power plants a steam accumulator is included to avoid a lack of steam in the event of the tripping of a refiner line etc. It further serves as a 'low pass filter' hindering fast steam variations from propagating into adjacent process areas.

To describe the differentiated forms of W_{TOT} and B_{TOT} with respect to the vector u, material and energy balances from the TMP must be derived as well. The dynamic changes in the vector elements in u can be seen as measurable inputs to an overall optimizer and are therefore straightforward to handle. However, the differentiated forms of W_{TOT} and B_{TOT} with respect to u are trickier to cope with. The major part of W_{TMP} is associated with the energy consumption in the refining processes, i.e. $W_{TMP} \approx \sum W_R$, where W_R is the electrical consumption in each refiner. As the modeling of the refiners is an essential step towards a better understanding of the process, the reader is referred to Karlström et al. (2008) and Karlström and Eriksson (2014a,b,c,d), where the extended entropy model is described in detail. It is important to mention that the entropy model is a physical non-linear model, which can still be used in on-line applications at sampling rates down to one second.

The differentiated forms of W_{TOT} and B_{TOT} with respect to the vector u can be formulated as

$$\frac{\partial W_{TOT}}{\partial u} = \frac{\partial W_{TMP}}{\partial u} + \frac{\partial W_{PM}}{\partial u} - \alpha \frac{\partial Q_{PP}}{\partial u}$$
$$\frac{\partial B_{TOT}}{\partial u} = \frac{(1+\alpha)}{\eta_P} \frac{\partial Q_{PP}}{\partial u}$$

where

$$\frac{\partial Q_{PP}}{\partial u} = \frac{\partial Q_{PM}}{\partial u} - W_{TMP} \frac{\partial \beta}{\partial u} - \beta \frac{\partial Q_{TMP}}{\partial u}$$

with β representing the steam efficiency[6], i.e.

$$\beta = \frac{Q_{TMP}}{W_{TMP}} \approx \frac{1}{n} \sum_{i=1}^{n} \frac{Q_{R_i}}{W_{R_i}} = 1 - \frac{1}{n} \sum_{i=1}^{n} \frac{Q_{loss_i}}{W_{R_i}}$$

where n is the number of refiners in the TMP mill[7].

The reason why these sets of equations are important to formulate is that W_{TOT} and B_{TOT} are directly related to the mill economy.

By introducing k_B and k_W as the cost of fuel and electricity, respectively, the total cost, K_{TOT}, can be defined as the sum of the power plant fuel cost, $k_B B_{TOT}$, and the cost of electricity, $k_W W_{TOT}$, in the TMP plant. By letting the ratio $\gamma = k_W / k_B$ be the relative cost between electricity and fuel, the total cost can be defined after differentiation as

$$\frac{\partial K_{TOT}}{\partial u} = k_B \left(\gamma \frac{\partial W_{TOT}}{\partial u} + \frac{\partial B_{TOT}}{\partial u} \right)$$

Thus, γ is a constant and therefore independent of the refiner control inputs. It depends on external conditions such as the market prices of electricity and fuel. As the market price in a near future will become variable over twenty-four hours, economic considerations for process optimization can easily be followed using this differentiated form.

Hence, combining the equations described above with an insight into the variations in γ and u is of the utmost importance for process optimization. However, to achieve improved energy efficiency in TMP processes, new strategies should be introduced where the emphasis is on the refiners to start with since they are directly associated with the pulp properties obtained at different operating conditions.

Certainly more aspects, such as investments in different types of refiners and the type of refining segments that the mill will use to reach a certain pulp quality, will affect the $\partial W_{TOT}/\partial u$ and consequently the complete economy. This will be commented upon several times in this series of papers.

Time scales: Most often the variations in the TMP variables described by the vector u have a substantial effect on the mill economy. By differentiating according to the equations above, the need to handle different time scales is highlighted. This is even more important to consider in time scales related to refining processes, see *Fig. 2*.

A time resolution of one millisecond to months must be analyzed to fully understand the refining process and how the fiber defibration/fibrillation in the refining zone affects the mill economy. For instance, different fluctuation phenomena caused by variable fiber distribution inside the refining zone can be analyzed with a time resolution of one minute, see Karlström and Eriksson (2014a), while changes caused by for instance variable raw material structure at different operating points requires a time resolution of about one hour. To study phenomena when the refining bars hit the fibers requires much faster sampling below one millisecond. Hence, all unwanted variations in vector u will affect W_{TOT} and consequently the total cost, K_{TOT}.

As steam generation is substantial in refining processes, the variations in B_{TOT} are not negligible. This is often overlooked and must be taken into account as well. However, in those cases where the power plants are optimized for production changes and run on a biomass related feedstock, the priority is to minimize W_{TOT}.

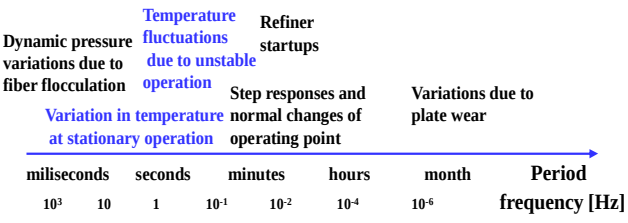

Fig. 2: Different time scales to be handled when running refining processes.

Different models have been suggested to cope with modeling techniques in refining processes. Karlström and Eriksson (2014a) derived an extended entropy model based on physical considerations in a CD refiner. The model, which is also called the Macro model, uses traditional process data such as production rate, hydraulic pressure applied on the refining segment holders (or plate

[6] It is noteworthy that, when a traditional enthalpy balance for the refining process is considered, an overestimate of the steam efficiency is obtained. About 5-7% of the total electricity consumption in a refiner relates to motor losses, heat radiation and irreversible work for defibration and fibrillation.

[7] Note that this is a theoretical description where no mal-functioning valves, power plant equipment etc. exist.

gap) and dilution water feed rate, i.e. the elements in vector u above together with the motor load and the temperature profile measured in the refining zone. The approach involves minimization of the difference between the motor load, W_L, and the computed refiner work, W_R, at different operating conditions. Here, the estimated total work is given by

$$W_R = \int_{r_{in}}^{r_{out}} 2\pi r w_R \, dr$$

and the distributed work is described by the relation

$$w_R = \alpha\mu(r\omega)^2 / \Delta(r)$$

Vector $\Delta(r)$ is the true distance between the refining segments (i.e. not only the plate gap in one position), ω is the angular speed of the refiner disc and r is the radius.

As the dynamic viscosity is most often unknown, the temperature profile and plate gap measurements are available as the free variables to find the product $\alpha\mu(T)$, see further Karlström and Eriksson (2014a).

This model is based on an entropy concept that handles both entropy and enthalpy balances depending on where in the refiners we study the process. This is illustrated in *Fig. 3*.

The main idea in this extended entropy model is to provide the split of the total work into thermodynamic work, which is related to the steam generation (i.e. the reversible work), and the irreversible work, which is related to the defibration/fibrillation work applied to the fibers, $w_{def}(r)$.

As the thermodynamic work is about 90-95% of the total work, a good estimate of the defibration and fibrillation of the fibers is essential if the focus is on fiber development. In cases where the steam generation is specifically considered, the total energy balance in TMP according to the derived mill-wide models also requires a good understanding of how to use the input variables described in vector u and their impact on the final mill economy.

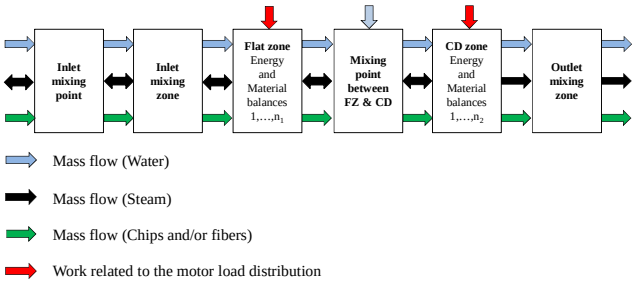

Fig. 3: Schematic description of the material and energy balances spanning a CD refiner.

One of the blocks, see *Fig. 4*, describes the energy balances in the flat zone, and this block is one of n_1 blocks that are set by the number of temperature sensors used in the sensor array (a complete list of equations and variable names is given in appendix A)[8].

[8] At first glance, the model seems to be rather complex, but off-line simulations indicate that the algorithms can be optimized for on-line applications in most process computers. It should be possible to include sampling rates down to one second. Much faster sampling rates can be handled if a parallel micro-processor is linked to the process computer.

Using the extended entropy model, it is possible to derive a rather good estimate of the average fiber residence time in different parts of the refining zone[9]. It is important to derive this variable if the fiber development is in focus.

The importance of residence time has been stressed by many e.g. May et al. (1987) and Härkönen et al. (1997). It is rather self-evident that the fiber can be developed only as long as they reside inside the refining zone. Härkönen et al. (1999) measured fiber residence time with radioactive tracers as a function of radius. Senger et al. (2005) and Vikman et al. (2005) published additional data based on measurements, and it is obvious from these papers that the earlier models by Miles and May (1990) are not able to predict a reasonable residence time.

The extended entropy model does not model local fiber recirculation in the refiner prior to the pressure peak but rather the residence time related to an uninterrupted fiber progress towards the periphery. Its usefulness in describing the fiber development is further explored below and, for the even faster dynamics related to the bar-to-fiber interaction the reader is referred to Appendix B.

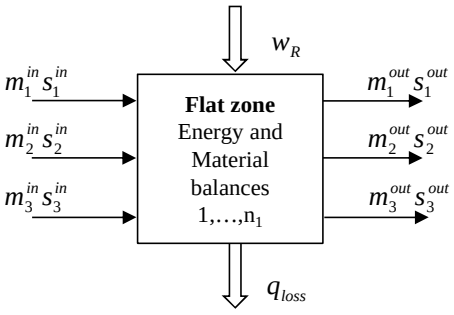

Fig. 4: Energy balance for a hypothetical refining zone.

As the fast dynamics are naturally linked to the slower dynamics[10], which directly relates to the macro-scale and the extended entropy model, it is essential to study process dynamics relevant for control purposes. In that sense the concept of residence time plays an essential role, which in the end affects the entire plant economy.

Results and discussion

Dynamics in refining processes are often overlooked in the literature (according to the introduction). This can be a consequence of the difficulties of simultaneously handling both the control concept design and a deeper process understanding.

Process conditions inside the refining zone are described by Karlström and Eriksson (2014a,b,c,d), and this paper focuses on the average residence time as a variable that should be used to describe the inherent nature of refining zone dynamics. This description must

[9] In this paper the fiber residence time and residence time will be equal if not specified otherwise.

[10] The fast dynamics are set by the rotational speed, machine and refining segment design.

be linked to a traditional understanding of refining zone dynamics in terms of plate gap, motor load and temperature profile variations, however, and a deeper discussion is therefore included in Appendix C as a complement.

The lack of a good modeling approach together with limited earlier information about machine and refining segment geometries made it difficult to get a grip on the residence time dynamics. The spatially dependent cross-sectional area occupied by pulp was especially difficult to extract using the old modeling approach derived by Miles and May (1991). Nevertheless, it is possible to extract the residence time in different parts of the refining zone using the extended entropy model given in Appendix A (see further Karlström and Eriksson (2014a)) if important machine parameters and refining segment geometries in combination with measurements of temperature profiles and plate gaps are available.

In high-consistency refiners, three phases or internal states exist simultaneously, i.e. dry wood/pulp, saturated water and saturated steam[11], denoted by subscripts {1,2,3} below[12].

As stated by Karlström and Eriksson (2014a,b,c,d), the estimated pulp dynamic viscosity is much higher than the dynamic viscosity for free water and steam during the defibration/fibrillation process, thus strengthening the assumption that the water is bounded to the fibers after the initial defibration of the wood chips at position r_{in}. It is therefore prudent to assume that the pulp and water velocities are equal, i.e. $v_1(r) = v_2(r)$, $r>r_{in}$.

The steam is known to move much faster than the pulp and water and it is possible to show this.

Example: Consider a CD refiner where the dry pulp density is set to 900 kg/m^3. The density for water and steam can be expressed by $\rho_{water}\approx -T+1065$ and $\rho_{steam}\approx 0.0747T-8.56$ within an interval of 140-180°C. The temperature profile is represented in *Table 1*.

The production rate of the refiner is assumed to be 12.5 T/h. The dilution water to the flat zone (FZ) is about 4 l/s and to the conical zone (CD) 3.5 l/s. The mass flows of pulp, water and steam inside the refining zone have been derived using the extended entropy model and process data from a commercial CD refiner[13], see *Table 1*.

The volumetric flow rates through a cross-sectional area inside the refining zone can be expressed by $V_i=m_i/\rho_i$ where $i=\{1,2,3\}$, i.e. for each component in the radial direction.

From these vectors it is obvious that $abs(V_3)>>V_2>V_1$. The volumetric flow of steam corresponds to about 90% of the total volumetric flow in the flat zone and about 95% in the CD zone.

In this example we assume that the depth of the grooves will be 3 mm in the flat zone for positions 6 to 11. The inner part of the segments, which corresponds to elements 4 to 5, is sparse in terms of bars. In this position only 10% of the surface consists of bars at the same time as the depth is variable.

Let the approximated depth $d(i)=f(R(i))$, where $R(i)$ is the radius from the refiner center, and estimate the components in the areas defined above. Assume a 2-mm depth in the conical zone for the stator and rotor segments. Without giving all details, this gives a set of cross-sectional areas calculated as described in *Table 1*.

Table 1: Variables used in the example: Note that the sensor position in the flat zone corresponds to the radius while the radius position in the CD zone is dependent on the angle between the flat zone and the CD zone.

Variable			1	2	3	4	5	6	7	8	9	10	11
Description	Name	Unit	Inlet			Flat zone							
Sensor position	r	mm				517	562	587	602	622	642	662	702
Temperature	T	°C	60	86	123	140	142	148	158	166	169	170	172
Fibre volume	V_1	m³/s				0,3							
Water volume	V_2	10^{-3}·m³/s				7,1	7,1	7,2	7,3	7,4	7,3	6,9	5,4
Steam volume	V_3	10^{-3}·m³/s				-172	-150	-132	-111	-94	-71	-20	20
Total cross-sectional area	A_{TOT}	10^{-2}·m²				11	6,2	2,4	2	1,7	1,8	1,9	2
Steam velocity	v_3	m/s				-1,6	-2,4	-5,6	-5,6	-5,4	-4	-1,1	10,2

Variable			12	13	14	15	16	17	18	19	20
Description	Name	Unit	CD zone								Casing
Sensor position	rx	mm	812	852	882	907	937	967	1002	1039	
Temperature	T	°C	173	171	169	167	166	165	162	160	146
Fibre volume	V_1	m³/s	0,3								
Water volume	V_2	10^{-3}·m³/s	10,9	10	9,2	8,4	7,4	6,3	4,8	2,9	
Steam volume	V_3	10^{-3}·m³/s	48,7	176	300	433	603	800	1119	1506	
Total cross-sectional area	A_{TOT}	10^{-2}·m²	1,6	1,7	1,7	1,8	1,9	1,9	2	2,1	
Steam velocity	v_3	m/s	3	10,5	17,2	24,2	32,6	41,7	56,8	73,5	

The area defined in the direction from the center of the refining segment to the periphery, see *Fig. 5*, can be described as $A_{TOT}(r)=A_C+A_{pp}(r)$, i.e. two cross-sectional areas comprising $A_C=2\pi r\Delta$, which describes the area between the bars and one that describes the area of the grooves $A_{pp}=2\pi r f(r)$.

The plate gaps, Δ, including the taper and the function $f(r)$ are plate pattern dependent and can vary considerably, see Karlström and Eriksson (2014a).

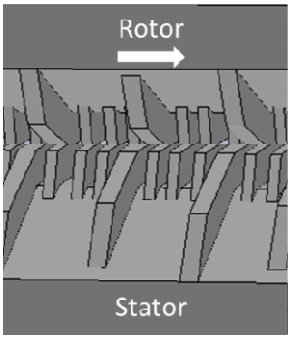

Fig. 5: Schematic drawing of the cross-sectional area, between two refining segments, consisting of the distance between the bars of the rotor and stator segments and the distance obtained from the grooves.

As the steam volume fraction dominates in all aspects, a relatively good estimate of the steam velocities at different positions in the refining zone can be obtained from $v_3\approx V_3/A_{TOT}$ - see further *Table 1* and *Fig. 6*. It is easy to conclude that the estimated velocity variations are largest in the periphery of the CD zone and, when the production rate reaches 15.8 T/hr, the vapor velocities approach nearly 200 m/s, which indicates that more fluctuations in the fiber pad must be expected, which can affect the final pulp quality. It is also fascinating to see that the open segment design in the inner part of the flat

[11] The wood/pulp phase describes dry material, i.e. dry wood near the inlet of the refiner and dry pulp further into the machine as the wood is defiberized.

[12] In low-consistency refiners, only dry wood/pulp and water exist, i.e. two phases, which simplify the physical modeling to some extent.

[13] For details, see Karlström and Eriksson (2014a,b).

zone so clearly lowers the velocity of the back flowing steam independent of the production level.

We will not go into a deeper discussion of the plate pattern design and its impact on the velocities in the refining zones, but instead prefer to continue and see if it is possible to find a good estimate of the residence time in the refining zone.

It is natural to assume that steam evacuation primarily follows the grooves. The amount of steam that follows the fibers into the contraction zone between the rotor and stator bars is therefore assumed to be negligible.

However, when the fibers are under contraction between the bars, the bounded water in the fibers is released as flash steam when the squeezed fiber pad is leaving the contraction zone.

The motivation is based on the visualized pressure fluctuations shown by Eriksen et al. (2008a,b). Karlström and Eriksson (2014c) showed by CFD modeling of the bar-to-fiber interaction that the temporarily increased pressure (2000-5000 kPa) between the bars is rapidly reduced when approaching the expansion zone in the grooves. The heat energy in the bounded water is thereby reduced to a level appropriate to the final saturated steam pressure, which can be obtained from the measured temperature profile. It is also natural to assume that free water leaving the contraction zone between the bars is evaporated momentarily when meeting the steam flowing radially in the grooves.

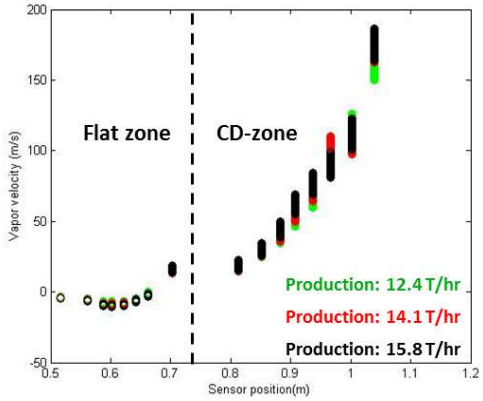

Fig. 6: Steam velocity versus the radius used in the entropy model for a CD refiner.

As a consequence of the discussion above we can formulate the following assumption, which follows the notation presented by Karlström and Eriksson (2014a,c):

Assumption 24: *The bounded water is released from the fibers during the expansion phase after the contraction region between the bars, and the fiber walls can thereby most likely be disrupted to some extent. It is assumed that the disruption is a part of the fiber fibrillation process caused by the thermo-dynamic work applied on the fiber.*

This type of defibration/fibrillation should not be associated with the irreversible work, which is strictly related to the mechanical work applied on the fibers via the shear forces between fibers and fiber bundles compressed between the refining bars.

The volumetric steam flow V_3 is much larger compared with the volumetric flows of pulp V_1 and water V_2 together, i.e. $abs(V_3)>>(V_1+V_2)$. From the extended entropy model it is shown that the vapor velocity v_3 is much larger compared with the pulp velocity v_1 in the refiner (see *Table 1*). As a result of that, the vapor is assumed to diffuse faster into the grooves compared with the pulp due to the tangential pressure drop as well as the radial pressure drop. The interplay between the tangential and radial pressure gradients is complex but is important to stress when discussing intricate fluid dynamics between the refining segments, which leads to the following assumption:

Assumption 25: *The volumetric steam flow is primarily localized to the grooves. The major part of the moving pulp, including the bounded water, will thereby be localized to the cross-sectional area between the bars and a hypothetical boundary layer between the stator and the rotor where the steam flow is not dominant.*

From the assumption $v_1(r)=v_2(r)$ the cross-sectional area for the water will be $A_2=A_1V_2/V_1$. Knowing the refining segment geometry, we also know the total cross-sectional area, A_{TOT}. The total volumetric flow V_{TOT} is known from the extended entropy model, see the discussion above. Together with the derived vapor velocity, which is much larger than the pulp velocity, i.e. $v_3(r)>>v_1(r)$, the cross-sectional area for the vapor

$$A_1 = \frac{V_1}{V_1+V_2}(A_{TOT}-A_3)$$

$$A_3 << \frac{V_3}{V_1}A_1 = \frac{V_3}{V_1+V_2}(A_{TOT}-A_3) \Rightarrow A_3\left(\frac{V_{tot}}{V_1+V_2}\right) << \frac{V_3}{V_1+V_2}A_{TOT}$$

$$A_3 << \frac{V_3}{V_{TOT}}A_{TOT}$$

However, $V_3 \approx V_{TOT}$, which means that $A_3 << A_{TOT}$, i.e.

$$\begin{cases} A_{1_{FZ}} \approx \dfrac{V_{1_{FZ}}}{V_{1_{FZ}}+V_{2_{FZ}}}A_{TOT_{FZ}} \\ A_{1_{CD}} \approx \dfrac{V_{1_{CD}}}{V_{1_{CD}}+V_{2_{CD}}}A_{TOT_{CD}} \end{cases}$$

As the residence time is expressed by the integral

$$\tau = \int_{r_{in}}^{r_{out}} \frac{1}{v_1(r)}dr = \int_{r_{in}}^{r_{out}} \frac{\rho_1(r)A_1}{m_1(r)}dr$$

the fiber development can be related individually to the flat zone and the conical zone, respectively.

Assumption 26: *The residence time, before and after the refining zone maximum temperature is assumed to be important, as is the total residence time, in the entire refining zone when describing the final pulp properties.*

The residence time varies a good deal along the radius and it is therefore natural to divide the flat zone into two different sets represented by the elements (position 1:2;

position 4:5 in *Table 1*) and the elements (position 3:8; position 6:11 in *Table 1*), see *Fig. 7*.

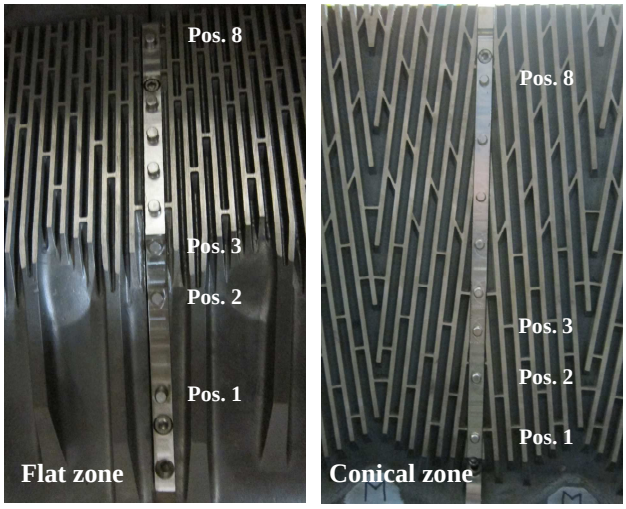

Fig. 7: Sensor arrays mounted between two segments in the flat zone (FZ) and conical (CD) zone. Eight positions for temperature measurements are indicated in both zones.

The reason is that the inner plate pattern represented by the elements (1:2) is sparse and open, while the rest, i.e. about half the total length of the refining segment, follow a more symmetrical distribution in terms of bars and grooves. The residence time of the mixture of chips and fiber bundles will be about the same for the inner interval 1 to 2 as for the interval 2 to 8, i.e. the region where the plate pattern is denser. This will be further commented below when studying the residence time ratio between the flat and conical zones. For the CD zone, with an almost identical plate pattern along the radius, the estimated residence time is supposed to not vary considerably as a function of radius. The inner residence time is even longer, however, as we do not count for the interval from the beginning of the segment to the first three positions defined in *Table 1*. In total, the residence time will probably reach about one second in the flat zone, and this calls for further research as this region stands for the defibration of the fibers and sets the conditions for further fiber development[14]. These statements will be discussed further below.

Specific energy and its relation to the residence time: The specific energy, i.e. the ratio between the motor load and production rate either as ADMT/h or preferably BDMT/h, is one of the most common variables used in the pulp and paper industry today despite the fact that pulp production is difficult to measure exactly. However, as an average, this measure gives a hint about the expected energy efficiency in the production line even though it must be used with caution when analyzing dynamic refining conditions inside the refining zone.

[14] It is worth mentioning that this region before the maximum temperature comprises a complex a mixture of chips, shives, fiber bundles and fibers of different sizes, which is certainly difficult to describe in details. However, it is important to understand the importance of this region for the final pulp property.

It is well known that changes in the manipulated variables, such as plate gap, dilution water feed rate and production, affect the specific energy and the residence time in the refining zone, and that leads us to the following assumption.

Assumption 27: *When the specific energy increases, the estimated total residence time increases as well.*

Consider the five different test series given in Table 2. The tests are performed during a period of three month and represent different process operating conditions.

Table 2: Mean values and the step/ramped changes in the plate gaps, dilution water feed rates and production.

Mean values	Unit	TEST1	TEST2	TEST3	TEST4	TEST5
Plate gap FZ	mm	1.5	1.3,0.9,1.3	1.2	1.5	0.9
Plate gap CD	mm	0.9	0.8	0.63,0.56,0.63	1.1	0.7
Dilution water FZ	l/s	3.3	3.4,3.1,3.4	3.8	3.4	3.3,3.55,3.3
Dilution water CD	l/s	4.8	5.2	5.1	3.9	4.7 , 4.4
Production	t/hr	13.5	15.3	15.8	12.4,14.1,15.8	14.5

In *Fig. 8* the specific energy is plotted versus the estimated total residence time in a CD refiner and it is clear that all test series fulfills the assumption.

It is also clear that all test series provide a huge amount of information depending on operating conditions etc. However, even though additional information about plate gaps, dilution water feed rates to the refining zones and production is given in *Table 2*, it is difficult and insufficient to analyze the conditions in each operating point only by studying the mean values. Further analysis must be made.

Moreover, as seen in *Table 2*, different step changes in the manipulated variables are performed in all test series except TEST1. This test series was included as a reference to study normal variations in pulp properties when the refiner was run at fixed set points.

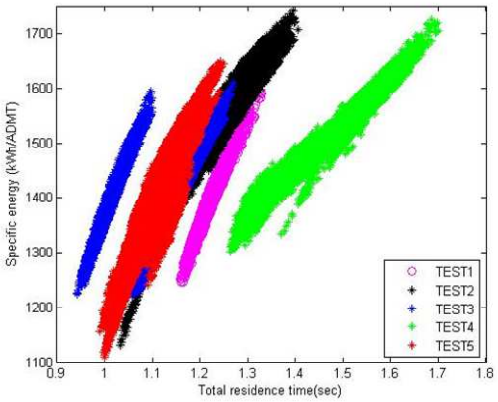

Fig. 8: Specific energy versus total residence time obtained from the extended entropy model.

As seen in *Fig. 8*, however, the specific energy varies between 1250 and 1550 kWh/ADMT for TEST1, and the question is whether something specific happens inside the refining zones which cannot be explained only by studying external conditions such as specific energy and other traditional input/output process data. This will be analyzed further below.

Since the extended entropy model is mainly based on the temperature profile and plate gap measurements, several distributed physical variables along the refining zone can be estimated. This means that local fluctuations in the residence time can also be analyzed.

Assumption 28: *To obtain lower specific energy, the ratio between the residence time in flat zone and the conical zone should be maximized.*

This assumption is hard to prove by using only external states such as specific energy, plate gap and dilution water feed rates to each refining zone. Not even knowledge of the internal state, i.e. the total residence time in *Fig. 8*, will help in the analysis. To understand more about the local fiber fluctuations in the refining zone we have at least to consider the residence time over the flat zone and conical zone, respectively, see *Fig. 9*.

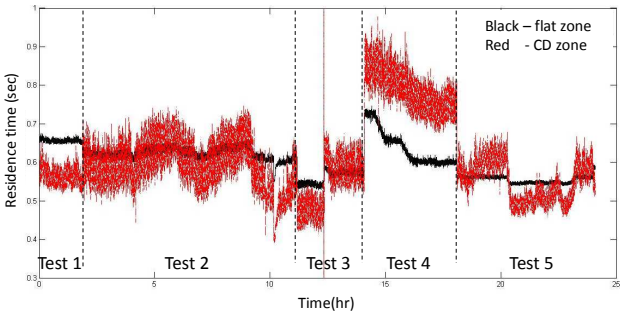

Fig. 9: Residence time in the flat zone and conical zone, respectively.

In TEST5, the prediction of the residence time in the conical zone is less accurate compared with the estimates in TEST1-TEST4 as the sensor array was not installed in the conical zone at the time. Fortunately, the sensor array in the flat zone was available and, knowing the temperature from the last sensor in the flat zone and the casing temperature, it is possible to derive a crude approximation of the residence time in the conical zone using the extended entropy model. From *Fig. 8*, it is clear that both TEST2 and TEST4 contain process conditions not so often used as a target in normal refiner operation. One reason for the high specific energy in TEST2 and TEST4 was that the consistency out from the flat zone is traditionally not estimated and thereby not possible to compensate for in the conical zone. Using the extended entropy model on-line, it is possible to overcome this problem, see further the discussion in Karlström and Eriksson (2014a,b,c,d). By using the extended entropy model, the motor load can be divided into work applied in the flat zone and conical zone. The time series in *Fig. 10* describe the relationship between the work in the flat zone and the motor load. Obviously, more than half of the work is carried out in the flat zone in all cases. During TEST4, around 65 % aligns with the long residence time in the flat zone compared to most of the other tests.

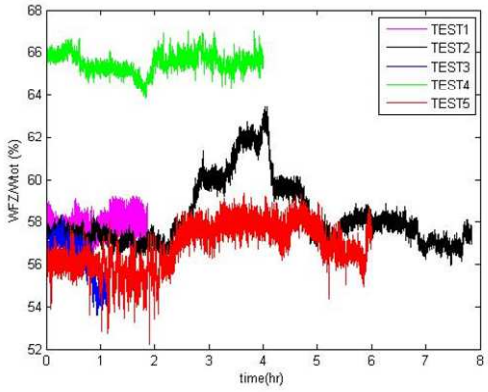

Fig. 10: The relation between the work in the flat zone and the motor load versus time for each time series.

It is also interesting to study the ratio between different variables, such as the work and the residence time, in FZ and CD. An inspection of *Fig. 11* gives an understanding of which test series to use in a deeper analysis if the relation between the residence times in each zone is in focus.

The ratio (R_{FZCD}) between the residence time in the flat zone and the conical zone is important according to assumption 28 as it gives an indication about the relative residence time in each zone. Thus, a ratio of $R_{FZCD}>1$ in *Fig. 11* and *Fig. 12* means that the residence time in the flat zone is larger than in the conical zone and, by plotting the specific energy versus R_{FZCD}, it is obvious that assumption 28 is strengthened for all test series.

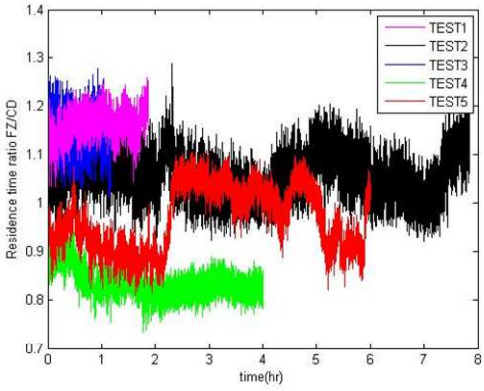

Fig. 11: Residence time ratio versus time for each time series.

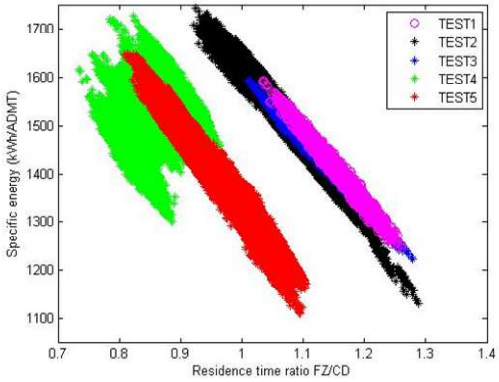

Fig. 12: Specific energy versus residence time ratio for each test series.

It is also notable in *Fig. 12* that the split between the residence times in each zone changes so much in TEST1, even though the manipulated variables had the same set points during the test.

Moreover, the process data from TEST1 and TEST3 are separated in *Fig. 8*, while overlapped in *Fig. 12*. This means that the residence times are equally increased in both zones in TEST3.

It is also important to mention that the residence time in each refining zone can vary as well. This is shown in *Fig. 13*, where the residence time obtained between the first two sensors (position 1:2) is divided by the residence time obtained for the rest of the segment radius (position 2:8).

The defibration is primarily assumed to take place in the first part of the flat zone, between positions 1 and 2, followed by a mix of defibration and fibrillation between positions 2 and 8. If the ratio $R_{FZ(1:2)FZ(2:8}>1$, the chips and fibers are assumed to stay longer in the inner part of the refining zone, which certainly affects the final pulp properties as the interaction between the fibers and the refining bars will vary considerably.

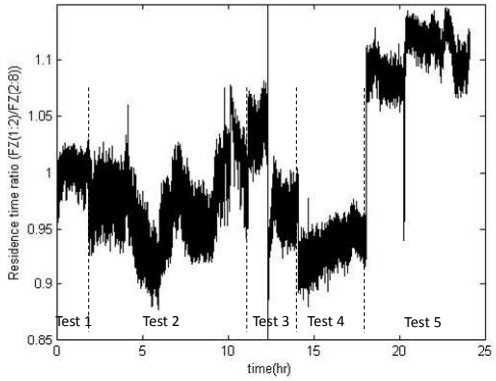

Fig. 13: Upper: Flat zone refining segment and sensor array positions used. Lower: Residence time ratio between sensor position 1:2 and position 2:8 in *Fig. 7*.

Specific energy and its relation to the work in the flat zone and the conical zone: The split of the motor load into the work in the flat zone and the conical zone respectively makes it possible to plot the specific energy versus the work ratio in FZ and CD, see *Fig. 14*.

It is interesting to see that the correlation between the specific energy and the work ratio is not as good as the correlation with the residence time ratio in *Fig. 12*, and that leads to the following assumption.

Assumption 29: *The estimated work ratio in the refining zones is not necessarily correlated to the residence time ratio.*

For simplicity, consider only TEST1 and apply a suitable low-pass filter on the entire data series in order to exclude some of the high frequency disturbances in the signals, see *Fig. 15*. By filtering, it is possible to visualize that the ratio between the total work in FZ and CD does not correlate with the ratio between the residence time in FZ and CD, see *Fig. 15*. This can also be estimated by using the correlation coefficient, which is about -0.05 and is only slightly improved to 0.25 if we alternatively only consider the defibration/fibrillation work defined by Karlström and Eriksson (2014a,b).

Hence, the residence time and the work distributed in the refining zones are not strongly correlated to each other.

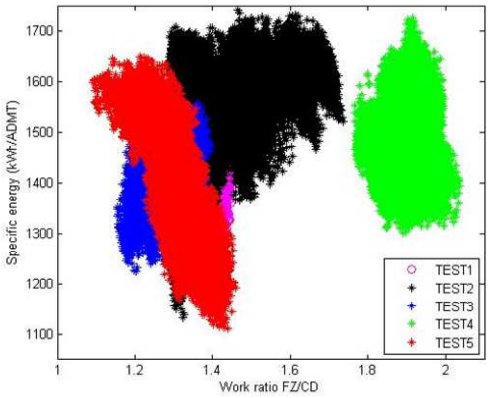

Fig. 14: Specific energy versus ratio between the flat zone work and the work in the conical zone.

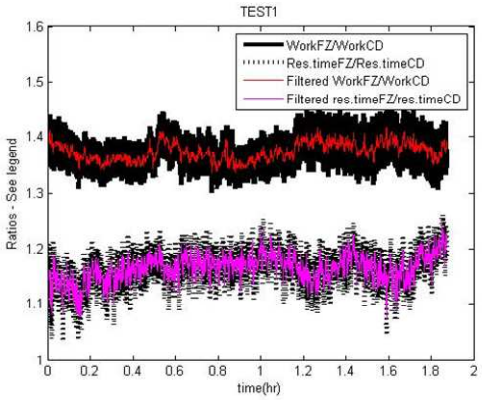

Fig. 15: Comparison between the work and residence time ratios in the flat zone and conical zone, respectively.

Total residence time and residence time ratio for different production rates: When studying *Fig. 8* - *Fig. 13*, it is clear that the sampling period in each test series is started at the process conditions at which the refiner is running at that time. This makes it possible to analyze the residence time in a broader perspective.

To approach the problem, it is natural to study the production levels during each test series. All process variables except the production are kept as stable as possible during TEST4, see *Table 2* and *Fig. 16*. Three production levels are significant, i.e. *{12.4, 14.1, 15.8}*, even though seventeen distinct levels are visualized in *Fig. 16* and *Fig. 17*.

As seen in *Fig. 17*, the total residence time is slightly reduced when increasing the production in TEST4 while the residence time ratio is kept quite stable during the trial.

Since the step changes in TEST4 are performed using a ramping procedure, each level can be followed in more detail when analyzing the total residence time versus the residence time ratio.

Assumption 30: *The residence time before and after the maximum temperature can differ depending on selected operating conditions.*

It is most likely that the fibers develop differently depending on how long they are kept in each zone. To get a deeper understanding of the nature of how to control the residence time, the residence time ratio can be plotted versus the total residence time, see *Fig. 18*.

By studying *Fig. 18*, it is seen that TEST4 has a long total residence time at the same time as the residence time ratio is relatively small. This means that the fibers are kept for a longer period in the conical zone compared with the flat zone.

Comparing *Fig. 16* and *Fig. 17*, it is clear that the assumed production rates in the test series are covered by TEST4. The major difference between i.e. TEST1 and TEST4 is related to the dilution water feed rate to the conical zone, see *Table 2*. This means that TEST1 in *Fig. 18* should be compared with the cyan colored data set between level 1 and level 9 in *Fig. 16* and opens for further studies.

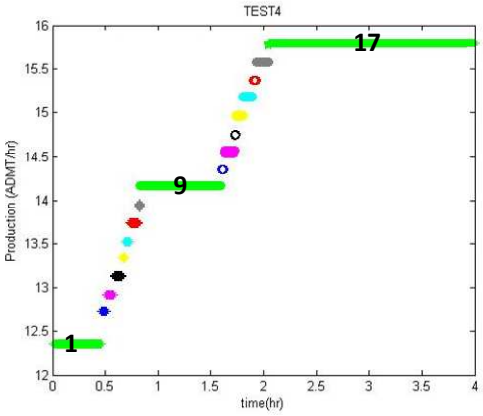

Fig. 16: Production versus time during TEST4.

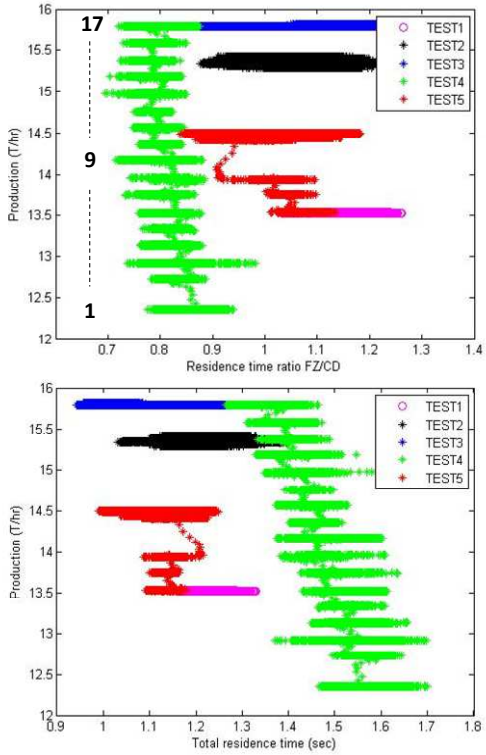

Fig. 17: Production versus total residence time and the residence time ratio for TEST1-TEST5.

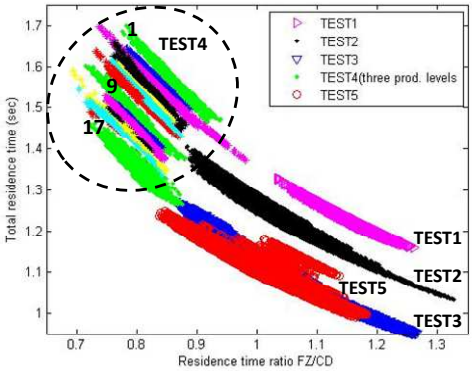

Fig. 18: Total residence time versus the residence time ratio.

Finally, additional information can be extracted by studying *Fig. 18* in combination with *Fig. 19*, where the residence time in the conical zone is plotted versus the residence time in the flat zone. This statement is based on the fact that each test series was started at normal process conditions, i.e. no process modifications were made in order to get a comparable starting point for each test series. This means that normal process operation is not based on prior information about how long the fibers are expected to stay in the refining zone to get an appropriate quality. Hence, this type of comparison opens a new field of possibilities to pre-specify the residence time in order to minimize process variation in a short-term and a long-term perspective.

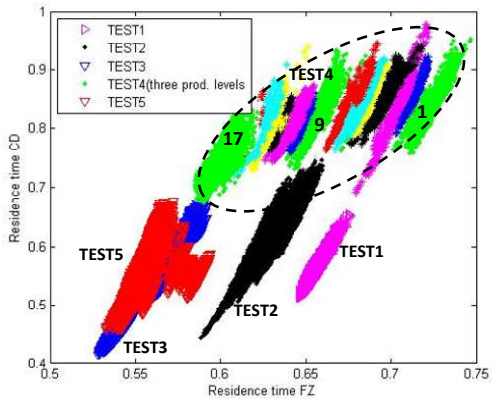

Fig. 19: Residence time in the conical zone versus residence time in the flat zone.

In a later paper in this series, a procedure to decouple and control the conditions in the refining zone will be derived. This implies that we can formulate vector *u* and thus link the conditions in the refining zone to the mill-wide energy perspective. It is also evident from Appendix C that the control system is limited to handling disturbances slower than an order of one minute. This calls for considerable care when designing the refining process considering that the fastest gap dynamics related to bar-to-fiber interaction exceeds 10 kHz.

Optimization of electrical energy usage in a pulp property perspective: In this paper we have not addressed the resulting pulp quality but rather shown that we can derive the conditions in the refining zone so that we can use the energy spent in a selected way. Thus there are inherent possibilities to translate pulp quality property

demands into residence time distributions and thereby temperature profiles. This will be addressed in a later series of papers building on the results of this series and the earlier series by Karlström and Eriksson (2014a,b,c,d).

Concluding remarks

Although the dynamics of the refiner imposes an extremely wide range of time scales, we conclude that we can describe the mill-wide material- and energy balances which leads to the conclusion that the cost optimization can be addressed in harmony with the pulp property demands as outlined earlier by finding the total paper production cost.

Furthermore, it has been shown that the control variables of the TMP refiners dominate the energy dynamics of an integrated newsprint or magazine paper mill. It is further deducted how the mill energy cost is related to these operating variables and current fuel and electricity prices.

It is also shown that the control variables of the TMP refiners need to fulfill the boundary conditions set by the required pulp properties of the produced paper grade. The pulp property development is strongly related to the residence time of the fibers in the refiner gap. The extended entropy model can be used to deduce residence time as a function of radius provided the refiner is equipped with temperature arrays in the refiner gap and a reliable disc clearance measurement.

We also state that stable and uniform refiner operating conditions promote both a uniform pulp quality and a stable electric energy demand. The refiner control variables can at best act on disturbances slower than one minute due to limitations in control valves, actuators and control loop performance. Faster variations have to be dealt with by proper process design of the refining system and the segments used.

This paper does not penetrate step changes caused by stop or start of any refiner line or paper machine. The economic optimization in such cases ought to be penetrated on a plant-specific level based on the formulas derived in this paper. An example of possible cost reductions due to improved refiner start-up procedures is given on the basis of data from a specific refiner.

Further, it is made clear that there is no way to decouple mill energy economics from the refiner performance and the pulp quality produced.

Finally, the following four papers elaborate on the control issues related to the application of the insights above to TMP refiner control. Furthermore, long-term results that have been achieved are presented and their impact on mill economy is explored in Paper IV in this series.

Acknowledgements

The authors gratefully acknowledge the funding by the Swedish Energy Agency, StoraEnso, Norske Skog, SCA and Holmen Paper. Special thanks go to Stora Enso Kvarnsveden mill for running trials and providing the excellent laboratory and process data used in this study.

Literature

Axelsson, E., Berntsson, T. (2005): Pinch analysis of a model mill: Economic and environmental gains from thermal process-integration in a state-of-the-art magazine paper mill. Nord. Pulp Paper Res. J 20(3):308-315.

Berg, D. (2005): A Comprehensive Approach to Modeling and Control of Thermomechanical Pulping Processes, Lic thesis. Dept. of Signals and Systems, Chalmers University of Technology, ISSN 1403-266x; nr R034/2005.

Dahlqvist G. and Ferrari B. (1981): Mill operating experience with a TMP refiner control system based on a true disc clearance measurement, International Mechanical Pulping Conference, Oslo, Norway, Session III, no. 6 (1981).

Eriksen, O., Holmqvist, C. and Mohlin, U-B. (2008a): Theoretical outline of the cause for observed cavitation in a low-consistency refiner, Nord. Pulp Paper Res. J 23 (3), 313.

Eriksen, O., Holmqvist, C. and Mohlin, U-B. (2008b): Fibre floc drainage-a possible cause for substantial pressure peaks in low-consistency refiners, Nord. Pulp Paper Res. J 23(3), 321.

Eriksson, K. (2005): An Entropy-based Modeling Approach to Internally Interconnected TMP Refining Processes, Licentiate thesis, Chalmers University of Technology, Göteborg, Sweden.

Eriksson, K. (2009): Towards improved control of TMP refining processes, PhD thesis, Chalmers University of Technology, Göteborg, Sweden.

R. Ferritsius, K. Eriksson, J. Hill, A. Karlström and O. Ferritsius (2014): Ch. 5 Exploring the potential for improved energy efficiency in wood chip refining processes by means of new measurement technologies: a CD82 refiner case study in Filling the Gap – Final Report (Eds. P. Engstrand, B.A. Engberg and K. Eriksson), FSCN report R-14-85, ISSN 1650-5387 2014:57

Hill, J., Westin, H., and Bergstrom, R. (1979): Monitoring pulp quality for process control, International Mechanical Pulping Conference, Toronto, Canada, p. 111-125.

Hill, J., Saarinen, K., Stenros, R.(1993): On the control of chip refining systems, Pulp and paper Canada, 94(6), 43.

Honkasalo, J.V., Polkkynen, E.E., Vainio,J.A., (1989): Development of control systems in mechanical pulping (GW, TMP) at Rauma, International Mechanical Pulping Conference, Helsinki, Finland, p. 376-389

Härkönen, E., Routtu, S., Routtu, A., Johansson, O. (1997): A theoretical model for a TMP-refiner International Mechanical Pulping Conference,Stockholm, Sweden

Härkönen, E., Huusari, E. amd Ravila, P.. (1999): Residence time of fibre in a single disc refiner, International Mechanical Pulping Conference, Houston, USA

Johansson B.-L., Karlsson H., Jung, E., (1980): Experiences with computer control, based on optical sensors for pulp quality, of a two-stage TMP-plant, 1980 Process Control Conference, Halifax, Nova Scotia, p. 145-152.

Jönsson, J. (2011): Analysing different technology pathways for the pulp and paper industry in a European energy systems perspective Ph.D thesis Chalmers University of Technology ISBN 978-91-73875-625-6 p 43-44

Karlström, A., Eriksson, K., Sikter, D. and Gustavsson, M. (2008): Refining models for control purposes, Nord. Pulp Paper Res. J 23(1), 129.

Karlström, A., and Isaksson, A. (2009): Multi-rate optimal control of TMP refining processes, International Mechanical Pulping Conference, Sundsvall, Sweden.

Karlström, A., (2013): Multi-scale modeling in TMP-processes, 8th Int. Fundamental Mech. Pulp Res. Seminar, Åre, Sweden.
Karlström, A. and Eriksson, K. (2014a): Fiber energy efficiency Part I: Extended entropy model. Nord. Pulp Paper Res. J 29(2), Pages 322-331.
Karlström, A. and Eriksson, K. (2014b): Fiber energy efficiency Part II: Forces acting on the refiner bars. Nord. Pulp Paper Res. J 29(2), 332.
Karlström, A. and Eriksson, K. (2014c): Fiber energy efficiency Part III: Modeling of fiber-to-bar interaction. Nord. Pulp Paper Res. J 29(3),401.
Karlström, A. and Eriksson, K. (2014d): Fiber energy efficiency Part IV: Multi-scale modeling of refining processes. Nord. Pulp Paper Res. J 29(3), 409.
Lafourcade, S., Labidi, J., Koteles, R., Gelinas,C.,Stuart,P. (2003): Thermal pinch analysis with process streams mixing at a TMP-newsprint mill Pulp and paper Canada 104(12): 74-77.
May, W.D., Miles, K.B., McRae, M.R., Lunan, W.E. (1987): An approach to the measurement of residence time in a chip refiner. International Mechanical Pulping Conference, Vancouver, B.B. Canada.
Noël, G. (1995): Pinch technology study at the Donohue Clermont newsprint mill. Pulp and paper Canada 96(7),38.
Miles, K. B. and May, W. D. (1990): The Flow of Pulp in Chip Refiners, J. Pulp Paper Sci. 16(2), 63.
Miles, K. B. and May, W. D. (1991): Predicting the performance of a chip refiner: A constitutive approach, International Mechanical Pulping Conference.
Oksum J., (1983): New technology in the Skogn mechanical pulp mill, International Mechanical Puling Conference, Washington DC, USA.
Rosenqvist, F., Eriksson, K. and Karlström, A. (2001): Time-variant modelling of TMP refining, Advanced Process Control Applications for Industry Workshop, Vancouver, Canada, 2-4 May 2001, IEEE Industry Applications Society, Vancouver, Canada, p 37-42.
Rosenqvist, F., Berg, D.,Karlström, A., Eriksson, K., Breitholtz, C. (2002): Internal interconnections in TMP refining IEEE Control Systems Society Conference on Control Applications', Glasgow, UK
Rosenqvist, F. (2004): Direction-dependent processes Theory and application PhD thesis, Chalmers University of Technology, Göteborg, Sweden.
Ruohonen, P., Ahtila, P. (2009): Analysis of a thermo mechanical pulp and paper mill using advanced composite curves. Proceedings of the 22nd International Conference of efficiency, Cost, Optimization, Simulation and Environmental Impact of Energy Systems, ECS, Foz duo Iguazú, Brasil..
Schaareman, M., Verstraeten, E.,Blaak, R., Hooimeijer, A., Chester, I., (2000): Energy and water pinch study at the Parenco paper mill Paper Technology 41(1),47-52.
Senger, J., Ouellet, D., Wild, P., Byrnes, P., Sabourin, M. (2005): A technique to measure residence time in TMP refiners based on inherent process fluctuations International Mechanical Pulping Conference, Oslo, Norway.
Vikman, K., Vuorio, P., Huhtanen, J-P., Huhtokari, J. (2005): Residence time measurements for a mill scale high consistency CD refiner line International Mechanical Pulping Conference, Oslo, Norway.

Appendix A

From the extended entropy model, it is possible to derive the forces acting on the fibers along the refining segments as well as the distributed consistency. This is a stationary model and is motivated from a perspective where the forces, obtained when the bars hit the fibers or fiber bundles, are averaged and derived using temperature profile information that follows the dynamics of steam. This information is fast compared with the control action that is possible to implement.

$$dS(r) = \frac{\delta(r)}{T(r)}\Delta(r)2\pi r dr$$

where

$$\delta(r) = \mu\left(\frac{r\omega}{\Delta(r)}\right)^2 = \frac{w_R(r)}{\Delta(r)}$$

We also know that

$$dS(r) = m_1 c_p \ln\left(\frac{T(r+dr)}{T(r)}\right) + \sum_{j=2}^{3}\left(m_j(r+dr)s_j(r+dr) - m_j(r)s_j(r)\right)$$

$$w_{th}(r)2\pi r dr = m_1 c_p (T(r+dr) - T(r)) + \sum_{j=2}^{3}\left(m_j(r+dr)h_j(r+dr) - m_j(r)h_j(r)\right)$$

which gives

$$\frac{w_R(r)}{T(r)}2\pi r dr = m_1 c_p \ln\left(\frac{T(r+dr)}{T(r)}\right) + \sum_{j=2}^{3}\left(m_j(r+dr)s_j(r+dr) - m_j(r)s_j(r)\right)$$

$$m_2(r) + m_3(r) = m_2(r+dr) + m_3(r+dr)$$

$$w_R \neq 0 \text{ and } q_{loss} \approx 0$$

$$m_1^{in} = m_1^{out} = m_1,\ m_2^{in} \text{ and } m_3^{in} \text{ are known} \Rightarrow$$

$$m_2^{in} + m_3^{in} = m_2^{out} + m_3^{out} \Rightarrow m_2^{out} = m_2^{in} + m_3^{in} - m_3^{out}$$

$$dr = r_{out} - r_{in}$$

Find m_3^{out}, $w_{th_{in}}$ and $w_{def_{in}}$

$$X = \frac{w_{R_{in}}}{T_{in}}2\pi r_{in} dr - m_1 c_p \ln\left(\frac{T_{out}}{T_{in}}\right) - m_2^{in}\left(s_2^{out} - s_2^{in}\right) - m_3^{in}\left(s_2^{out} - s_3^{in}\right)$$

$$Y = m_1 c_p (T_{out} - T_{in}) + m_2^{out} h_2^{out} - m_2^{in} h_2^{in} + m_3^{out} h_3^{out} - m_3^{in} h_3^{in}$$

$$m_3^{out} = X / \left(s_3^{out} - s_2^{out}\right)$$

$$w_{th_{in}} = Y / (2\pi r dr)$$

$$w_{def_{in}} = w_{R_{in}} - w_{th_{in}}$$

Table 1: Latin symbols

Symbol	Description
c_p	Heat capacity
dS	Entropy genertion
h_i	Specific enthalpy of component *i*
m_i	Material of component *i*
q_{loss}	Energy losses per unit area
r	Radial coordinate
s_i	Specific entropy of component *i*
S	Total entropy
T	Temperature
w_{th}	Thermodynamic work per unit area
w_{def}	Refining work per unit area
w_R	Estimated total work per unit area

Table 2: Greek symbols

Symbol	Description
δ	Viscous dissipation
μ	Dynamic viscosity
ω	Angular speed of the refiner disc
Δ	Plate gap at radius *r*

Table 3: Indices

Sub-&Superscript	Description
1	Wood/Pulp phase
2	Water phase
3	Steam phase
in	Refiner inlet
out	Refiner outlet

Appendix B

Computational fluid dynamic models can be used to study the refining bars' impact on the fibers. This was showed by Karlström and Eriksson (2014c) using a set of Navier-Stoke equations

$$\rho\left(\frac{\partial \mathbf{v}}{\partial t}+\mathbf{v}\cdot\nabla\mathbf{v}\right)=-\nabla p+\nabla\cdot\mathbf{T}+\mathbf{f}$$

where ρ is the fluid density, $\mathbf{v}$ is the flow velocity and p the pressure, see Karlström and Eriksson (2014a,b,c,d), ∇ is the del, $\mathbf{T}$ is the stress tensor and $\mathbf{f}$ represents the body force[15] per unit volume acting on the fluid (such as gravity and centrifugal forces). Hence, the left side of the equation comprises the unsteady acceleration[16] and the convective acceleration[17], while the right side represents by the pressure gradient, shear and body forces.

This model was called the micro model, as the focus is on the bar-to-fiber interaction. The fluid mechanics inside the refining zone is directly dependent on the elements in vector *u*, as shown by Karlström and Eriksson (2014,d).

Dynamic responses caused by bar-to-fiber interaction can be illustrated by fast sensors mounted on the surface of a bar, and several types of sensors can be used, see Karlström and Eriksson (2014c,d). This paper focused on dynamic pressure measurements as these directly relate to the Navier-Stokes equations see Karlström and Eriksson (2014c). It is important to stress that fast dynamics is essential to handle in refining theory as it sets the fingerprint of pulp characteristics. However, these types of process dynamics are difficult to control on a micro scale. Nevertheless, the fluid dynamics between the refining segments affect the fiber distribution and steam clearance, which are indeed important to control on a macro scale. Some information about the fluid dynamics is given below, but the reader is referred to Karlström and Eriksson (2014c) for a deeper discussion of pulp acceleration, retardation and various pulp viscosities etc. along the refining zone radius.

Fig. 20 shows two different sets, comprising 4000 samples each. These sets of pressure fluctuations are obtained from a full-scale refiner and describe how the refining bars hit the fibers and fiber bundles.

The pressure was measured using a fiber-optic Fabry-Perot interferometer (sampling rate; 8 µsec.) at the same position at different plate gaps. In the first series, 1, corresponding to a large gap[18], the temperature was about 162°C while in series 7, with a smaller plate gap the temperature was about 171°C. The other series in between (not shown in this paper) corresponds to an intermittently reduced plate gap. As seen in *Fig. 20*, it is clear that a large plate gap tends to allow larger fiber bundles to cross the leading edge of the bars while a smaller plate gap gives a more homogeneous mixture with smaller fiber bundles between the refining bars. The increased temperature when reducing the distance between the rotor and stator in the refiner studied will also affect the pulp viscosity and thereby affect the softening of the fiber bundles. This will change both defibration and fibrillation of the fibers. The increased bar-to-fiber impact when reducing the plate gap is best visualized in a histogram, see *Fig. 21*.

The histogram in *Fig. 21* covers the first two series and the last two series. It can be concluded that the spread in pressure peaks is significant. Series 1 and 2 correspond to the sets with a larger plate gap as compared with series 6 and 7. The large plate gap will result in lower impacts per bar, and that will consequently result in a larger population for series 1 and series 2 in the low pressure peak regions in *Fig. 21* compared with the curves representing series 6 and 7, which have much more pressure peaks in the upper region, i.e. the right hand side in *Fig. 21*. On the x-axis, the estimated normal force is included in order to show that the pressure sensor can be used as a shear soft sensor as well.

The phenomena obtained by measuring e.g. dynamic pressure and/or shear forces between the refining bars are of course related to fast dynamics. Such measurements are useful for analysis of the bar-to-fiber impacts and depend on changes in vector u, as seen in *Fig. 21*.

Only plate gap changes have been studied to date, but it is believed that both production and dilution water feed rate will affect the distribution described by the histogram

[15] The body force acts throughout the volume of the body (such as gravity) which is different from the traditional contact force.

[16] This type of acceleration is also called the local rate of change and describes the variation of **v** in time at a specific position.

[17] Corresponds to the convective rate of change and describes the variation of **v** in space when the fluid passes a specific position.

[18] It was not possible to detect the absolute plate gaps during the tests. Instead, the hydraulic pressure, *h*, in the vector *u* was used to control the distance between the refining segments.

in a similar way. This can especially be used when optimizing in different research applications, e.g. as input to the Navier-Stokes equations given above and future refining segment designs, see further Karlström and Eriksson (2014c,d). To use such information for control purposes, the pressure measurements must be implemented on a sensor array covering the entire refining zone and have to be used on an average basis as the actuators are much slower. The average fiber energy distribution has so far not been used in any optimization tools coupled to economic studies at different operating conditions.

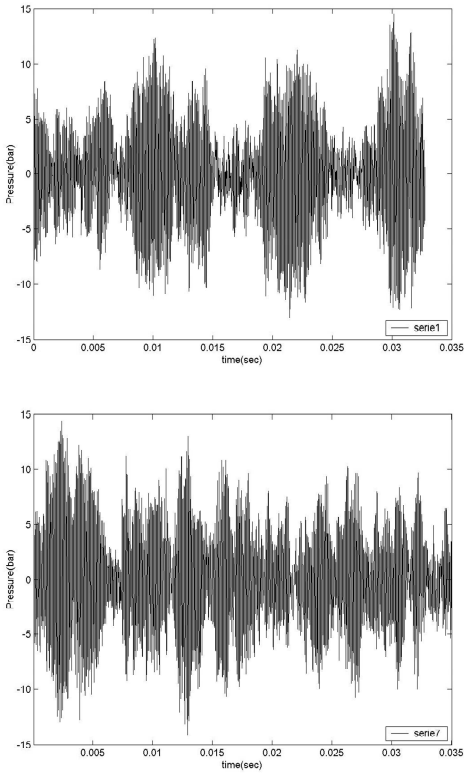

Fig. 20: Upper: Close-up of pressure response for production with a large plate gap (Series 1). Lower: Close-up of pressure response with a smaller plate gap (Series 7)[19].

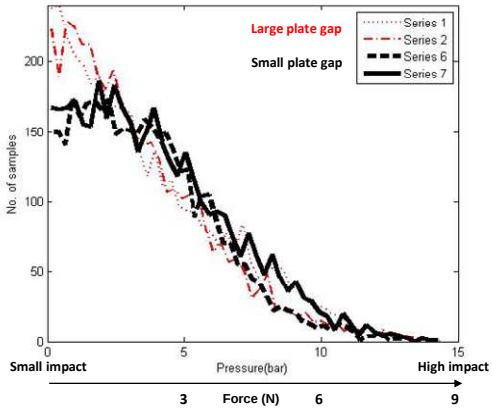

Fig. 21: Histogram describing the distribution of the pressure for series 1 and series 2, which is captured using a larger plate gap compared with series 6 and series 7, which have a smaller plate gap.

[19] In cooperation with Norske Skog ASA, Research and Follum mill.

Appendix C

Process design and actuator related dynamics: The individual refiner is controlled by the production rate (P), hydraulic pressure (h) and dilution water (D) forming the vector u. There are two additional control variables: inlet pressure (p_{inlet}) and casing pressure (p_{casing}). There may also be seal waters serving both transport screws and the refiner itself and possibly also post-refiner dilution water. The dynamic characteristics of these control loops are not described in the literature except in Rosenqvist's thesis (Rosenqvist, 2004). In most mill-specific process studies, it is essential to establish the characteristics of these loops. The following dynamic data is a summary of results from some 20 process studies in more than a dozen TMP mills carried out for individual customers over the years.

Production rate (P) is almost always set by a metering screw, either a plug screw or an atmospheric or pressurized metering screw. These screws are usually driven by an electric motor supplied from a variable frequency drive. If the motor and drive are properly sized and tuned, the time constant of a production rate change is in the order of 1 - 3 seconds. This is negligible compared to most other time constants outlined below. From the metering screw to the entry of the refiner gap, there is a dead-time which is determined by the transport screw set-up of the individual production line. A typical value of the time lag is 8 s.

Hydraulic pressure (h) is used in most refiners to adjust the gap. There are some exceptions, e.g. Jyhlä single disc refiners and the flat zone of CD refiners, which are controlled by mechanical devices. In the case of most Metso manufactured refiners, the control valve adjusting the hydraulic closing and opening pressures is mounted along the refiner shaft and is controlled directly by refiner shaft movements. Its position along the shaft can be altered manually or automatically in order to execute different gap set points. Andritz' hydraulic pressure control is designed as a separate control valve acting on the closing and opening pressures of the hydraulic cylinders' actuating gap movements. The control valves are very fast compared to all other actuators used to control refiner variables. The performance differs with regard to disturbance rejection, as pointed out by Dahlqvist et al. (1993). In practice, the time constant of the pressure controller is set by Newton's force equation provided that the system is friction free – both friction and stiction may occur in the real system.

$$\partial^2 x/\partial t^2 = F_{tot}/m,$$

where x is the refiner disc position [m], F_{tot} force [N] and m mass [kg].

In most mill cases, force F_{tot} cannot be measured or calculated. It is the sum of the hydraulic pressure action on the gap controlling cylinders creating a hydraulic force F_{hydr}, the casing pressure p_{casing} acting on the rotor area A, minus the steam pressure $p_{refiner}(r)$ acting inside the

refining gap and minus the force carried by the pulp $F_{pulp}(r)$.

$$F_{tot} = F_{hydr} + A \cdot p_{casing} - \int p_{refiner}(r)dr - \int F_{pulp}(r)dr$$

When operating at the desired set point, F_{tot} is supposed to be zero. When a change in the gap is required, all terms will be impacted but the casing pressure, if properly controlled. The rate of change is in most cases directionally dependent as it is harder to close the gap than to open it under normal operating conditions – see Rosenqvist et al. (2001), who report time constants under normal refiner operation in the range of 1 min. of the refiner studied. Start of refining and stop of refining add two important cases that deserve particular attention when designing the control schemes in order both to protect the segments and to ensure proper pulp quality. In these cases the force generated by the hydraulic pressure is the dominating one and thus the rate of movement is strongly related to the inertia created by the mass to be moved.

Dilution water flow-rate control has a typical dead-time of 4 to 10 s and a time constant 5 to 20 s. The performance of this control loop is strongly linked to the process design and the choice of valves and actuators. Normally, the dilution water is fed from a high pressure pump (> 1 MPa) into the inlet of the refiner at a substantially lower pressure, typically < 300 kPa. The intention is that the pressure drop variation from the high pressure pump to the exit of the nozzles in the refiner shall be very large compared to the short-term variations of the inlet pressure, thus minimizing dilution water flow rate disturbance. In many designs, a clack valve is included to prevent nozzle clogging, which can cause rather random types of disturbance patterns of the flow rate.

The inlet pressure control loop has a typical dead-time of 4 to 12 s and a time constant 8 to 30 s. The time lag and time constant are strongly linked to the process design. There are two extremes:

- Chips entered into a small volume to the refiner with steam venting to an appropriate steam header offering the fastest responses
- Steam vented into a pre-heating vessel and the inlet pressure controlled in the total volume of this vessel and the succeeding volume until the entry of the refiner. Naturally this leads to slow response characteristics.

The casing pressure control loop has a typical dead-time of 4 to 20 s and a time constant of 8 to 40 s. This control suffers from the conflict of start-up performance and precision during continuous operation. In many cases the performance is poor in both cases due to the compromise of using only one large valve handling typically 4 to 8 kg/s of steam with a velocity of typically 25 m/s. In addition, the process inter-connections formed by the refiner itself tend to cause interference between the dilution water controller and the casing pressure controller. The oscillations in these controls reported by Rosenqvist et al. (2002) are not unusual in TMP production lines. In many cases the tuning of the loops will not solve the problem without degrading loop performance but tend to call for process design changes in order to achieve both good and robust control.

The control of various seal waters is often carried out by hand valves set in fixed positions. Considering that there may either be many seal waters to support or designs demanding large amounts of seal water, this water can in the extreme approach half of the dilution water flow rate. Naturally this design is not acceptable in the first place. In some cases there is a differential pressure controller between the inlet pressure and the outlet pressure of the seal water pump to improve their performance. It is still doubtful as to whether this offers performance on an acceptable level from a refiner performance control perspective. However, the focus has been directed more toward improving e.g. mechanical seal performance than to improving the performance of installed sloppy seal water controls.

In summary, the currently used process designs and controls will not allow for a faster refiner control than 1 min or less frequently. It should be obvious from this review of the typical performance of loops that there is substantial room for both loop performance improvements and reduction of the general process noise levels if a more stringent control perspective had been applied to the process design and the selection of control equipment.

Below, as an example, CD refiner dynamics will be penetrated in order to give the reader insight into which variables should be considered when new control concepts are formulated.

Normally, the feeding screw in a CD refiner is synchronized with the dilution. The start-up procedure ramp is about 10 seconds and the plate gap is not controlled until the process reaches a stable production and is therefore increased together with the motor load due to the forces acting on the refining segment surface.

That the plate gap responds in the same direction as the motor load when changing the production is clearly visualized in *Fig. 22*.

When a stable production is reached and no changes in dilution water feed rate occur, small disturbances in the chip feed rate from the feeding screw can still affect the plate gap dynamics, as shown in *Fig. 23*. This situation is not unusual in spite of the fact that the plate gap control system is in automatic mode as the dynamics cannot be handled by the actuators. If the disturbance in the feeding screw affects the production level, in the long run the plate gap will be controlled back to the original set point.

If the disturbances in the chip feed rate are slower and larger in magnitude, there will be a considerable influence on fiber distribution in the refining zone, see Karlström and Eriksson (2014b). This means that the refiner does not operate properly, which can ultimately can have an impact on the final energy economy and pulp properties.

As shown by Karlström and Eriksson (2014b), the temperature responses in the flat zone and CD zone differ from each other; moreover, it is shown that the energy balance in each zone has local fluctuations. This means that the temperature response from each sensor, at different radius, does not necessarily coincide with the

motor load. The motivation for this statement is that the dynamics in the distributed work $w_R(r)$ depends on how the fiber distribution is built up. This is also the reason why the extended entropy model is described as a set of stationary equations.

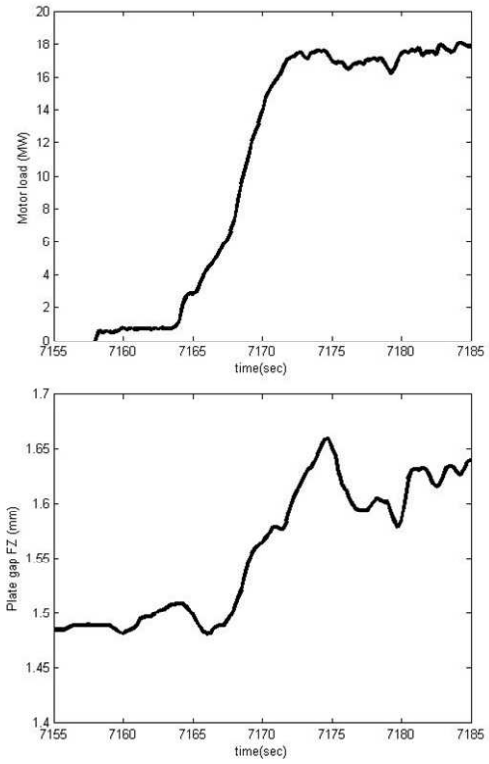

Fig. 22: Motor load and plate gap changes obtained when starting up a CD refiner.

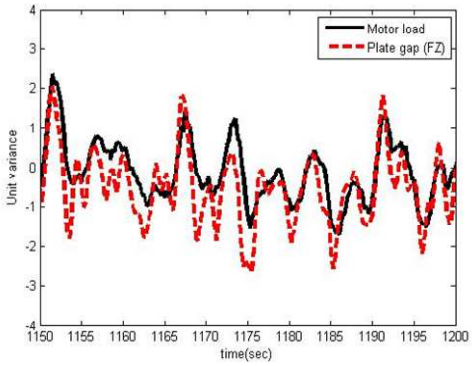

Fig. 23: Unit variance in motor load and plate gap in the flat zone (plate gap control in automatic mode).

All dynamics refers to input vector u. The internal states $T(r)$ and the outputs such as motor load W_L and pulp properties are considerably affected, and it is essential to filter the fast dynamics to prepare the data set for further comparison on the same time scale. This is easy to understand by studying the different dynamics in the flat zone and CD zone. As illustrated in *Fig. 24*, the temperature profile response in the flat zone (represented by the 8th sensor, biased -100°C) seems to be delayed. The temperature profile in the CD zone, represented by the 8th sensor, biased -100°C, responds momentarily.

The temperature time constant in the flat zone is larger than the time constant in the CD zone. This is a consequence of the fact that both water and steam are moving in the same direction as the pulp in the CD zone, which affects the residence time and thereby results in a smaller time constant. The process inside the flat zone comprises a more intricate balance between the water flow, which follows the same direction as the chips/pulp and the backward flowing steam.

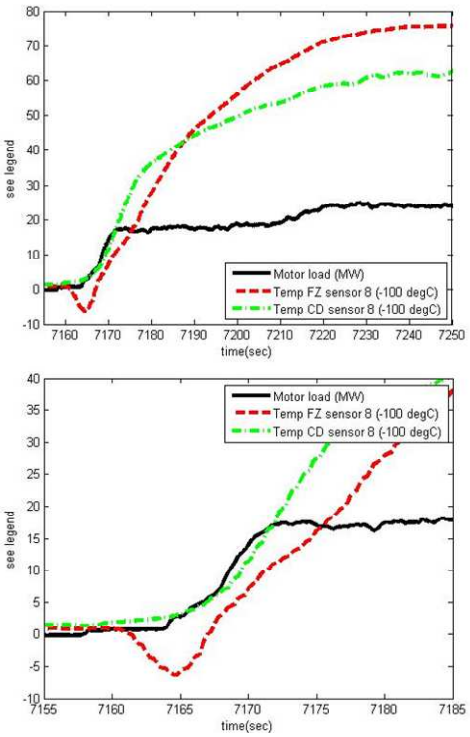

Fig. 24: Response in motor load and temperature in the flat zone and CD zone during start-up – two different time resolutions.

It is worth mentioning that the temperature delay in the flat zone shown in *Fig. 24* is sometimes negligible. The time constant seems to be similar, independent of the start-up procedure.

From an external perspective, when temperature sensor arrays are not available in the refining zone, these phenomena are difficult to analyze. In summary, we can conclude that all start-up procedures are individual and the fiber network obtained will be different from time to time, even though the same plate gap is obtained.

The motor load responds momentarily while the temperature response depends on the distributed fiber packing degree of the viscous pulp. A high local fiber packing degree tends to increase the steam generation locally. Therefore, we need to find the delays and which filter should be used for the motor load before comparing it with the temperature profiles in the flat zone and the CD zone.

By comparing the correlation coefficient at different delays and low-pass frequencies, it is possible to find the optimum, see *Fig. 25*. Here, 1000 samples with a sampling rate of 4 Hz were analyzed for a period where the refiner ran for several hours after start-up. In this specific case, the delay is about 5 seconds and the low-pass filter frequency about 0.09 Hz, i.e. a frequency corresponding to an 11-second low-pass filter. As the

square of the coefficient (or **r** square) is equal to the percent of the variation in the motor load that is related to the variation in the temperature (3rd sensor), an **r** of 0.8 means that 64 % of the variations is related to this third sensor in the flat zone.

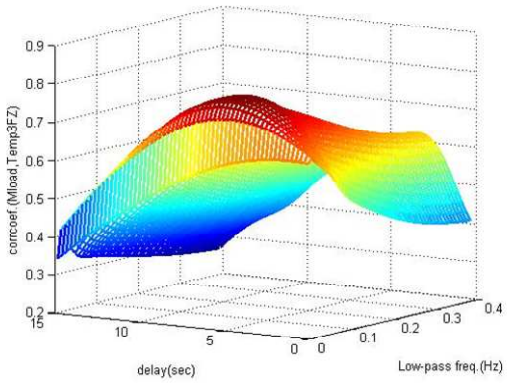

Fig. 25: 3D plot of the correlation between the motor load and the temperature in the flat zone, here represented by the 3rd sensor.

Even though the correlation is sufficiently high for this time series, the situation can change dramatically due to local fluctuations in the fiber network. In other words, a small fluctuation that results in a better response for another temperature sensor cannot be captured by comparing the responses in motor load and the 3rd temperature sensor only, see the discussion in Karlström and Eriksson, (2014b). Instead, the motor load must be compared with several temperature sensors to capture how the fiber network has been changed to get similar value of **r** as above[20]. However, in general, a low-pass filter of 10-15 seconds will do fine.

The temperature responds in the same direction as the motor load according to *Fig. 25*, and plotting the motor load and the biased temperature from the 3rd sensor for a longer period gives acceptable results as well, see *Fig. 26*.

We can conclude that an increased production due to a disturbance in the feeding system will increase the motor load and the plate gap. If the temperature profile is raised as well, this is an indication of an increased degree of fiber packing. In other words, for process conditions where a positive correlation between the temperature and the plate gap exists, a new operating point (and most likely also the pulp defibration/ fibrillation) is obtained.

Note that this dynamics can be obtained in the refining zone only when the chip or pulp feed rate is changed to the refining zone.

It is noteworthy that an increased dilution water feed rate to the refining zone, see *Fig. 27a*, will result in a lower temperature before and a higher temperature after the maximum temperature. This is a consequence of the cooling effect from the incoming dilution water, while it also results in a higher steam production that increases the temperature in the periphery of the refining zone. It has completely to do with backward and forward flowing steam, see further the discussion in Karlström and Eriksson (2014a,b,c,d).

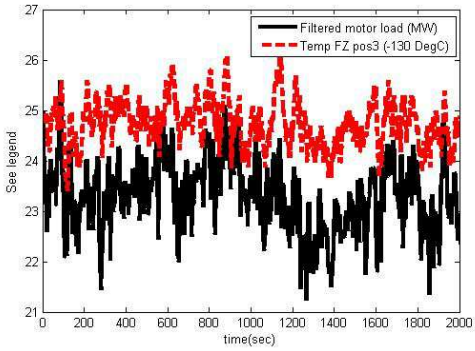

Fig. 26: Comparison between the motor load and the biased temperature (-130 °C) for a time series of 8000 samples.

When making a deliberate change in the plate gap by manipulating e.g. the hydraulic pressure, the correlations between the plate gap and the motor load or the temperature profile become negative. In other words, the temperature profile[21] responds differently when applying a positive step change in the dilution water compared with those in production and plate gap (hydraulic pressure), see *Fig. 27*.

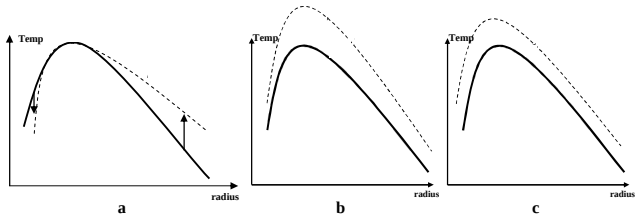

Fig. 27: Temperature responses versus radius when applying positive step changes to a) the dilution water b) the plate gap (hydraulic pressure) and c) chip and pulp feed rate.

When reducing the plate gap, done by increasing the hydraulic pressure on the holder, the temperature profile will be lifted to another position, as described in *Fig. 27b*. Increased production will act in the same direction as when changing the plate gap, i.e. lift the temperature profile to a higher level[22] as seen in *Fig. 27c*.

Much more can be said about the temperature profile dynamics and in *Fig. 28* a 3D-plot for the temperature profile near the maximum is given as an example. The production is increased in two steps according to Karlström and Eriksson (2014b) without changing the Dilution water. Near the production limitation the sensors in the periphery of the CD-zone will fluctuate considerably. This phenomenon will cause undesired fiber shortening and should be avoided.

[20] The reason why we show this is that the weighting vector used by Karlström and Eriksson (2014b) must be handled with care as the time constants in the temperature responses will change dependent on the process conditions.

[21] The responses are schematically visualized and differ to some extent regarding the spatial gains for different segment designs. In most refiners so far studied the differences are negligible.

[22] Sometimes a change in the production rate affects the position for the temperature maximum. This is certainly true near process limitations.

The temperature increase in the periphery of the CD-zone is not seen in the specific energy[23], see *Fig. 29*. This is interesting from many aspects and is penetrated in details by Karlström and Eriksson (2014a,b,c,d).

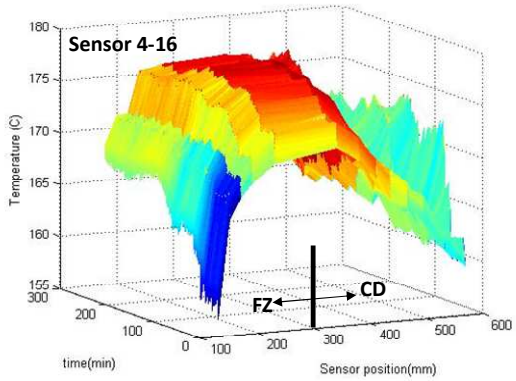

Fig. 28: 3D-plot of the temperature responses at the periphery of the flat zone (100-250 mm) and the entire CD-zone when performing production changes.

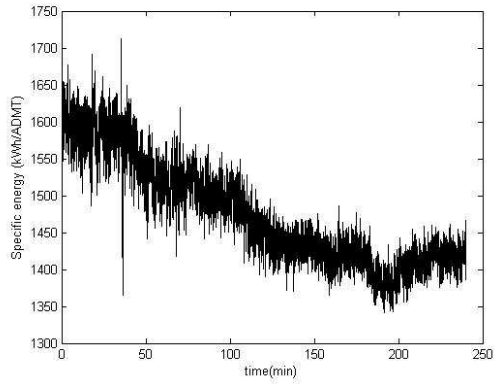

Fig. 29: Specific energy versus time when increasing the production.

The control design and actuator dynamics are essential in all processes and often overlooked in research literature. However, often the entire process design inhibits the possibilities to revamp the system. In order to cope with the process design and actuator related dynamics some of the important issues are included in Berg (2005).

In summary, the fact that the elements in the vector *u* affect the dynamic fluctuations in the defibration and fibrillation work inside the refining zone makes it relevant to introduce a more rigorous control concept. This will be penetrated in more details later in this series of papers.

Start-up procedures: To link the mill economy to the TMP process it is natural to perform long term follow up of different process conditions. This is a tedious work and a new approach will be presented later in the series of papers. Instead, as an example we choose to study refiner start-up procedures. Most often it is performed manually by the operators and this gives an opportunity to consider different start up strategies and their impact on the process economics. The control system is placed in automatic mode after about ten minutes from start when the process is stable enough and runs without any problems. How to control the vector u to get the most optimal start-up without major impact on the economy in terms of electricity cost and acceptable pulp quality is a challenging task.

To study the start-up procedures it is convenient to introduce a segmentation of the data series, i.e. a split of the data series to cover each start-up procedure, in order to minimize the data set to be studied. This can be done on a yearly basis and a segment horizon of +/- one hour is good enough for a process follow up[24].

The segmentation of data is shown in *Fig. 30* where the hydraulic pressures from a complete production line are shown for some typical start-up procedures during two days. It easy to see how different the start-ups are performed and of course this will affect the pulp quality considerably.

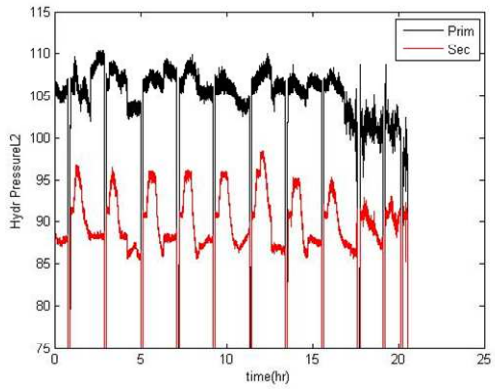

Fig. 30: Hydraulic pressure for two serially linked Twin refiners, one primary (Prim) and one secondary (Sec) refiner.

In many situations the operators decide to start up the production by loading the refiners as much as possible, see *Fig. 31*, and an over shoot of 2-3 MW is not an unusual situation. This, however, means that a settling time of about one hour is expected before decided process condition is obtained even though the control systems are set in automatic mode after ten minutes.

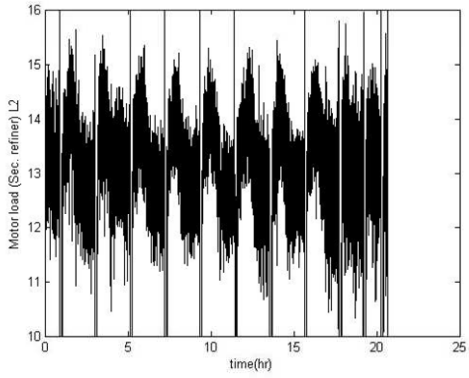

Fig. 31: Close up of the motor load for the secondary refiner.

As described by Karlström and Eriksson (2014b), the fiber distribution which can be indirectly described by the

[23] The specific energy is defined as the relation between refining energy consumption and the assumed production rate.

[24] In this example, the segmentation covers one hour before and one hour after the start-up trials.

temperature in different positions along the refining segment radius will vary much dependent on the refining zone conditions. This is shown in *Fig. 32*, where the sensor 4 and sensor 6, with a position 95 mm and 150 mm respectively, shift in magnitude during some of the start-up procedures.

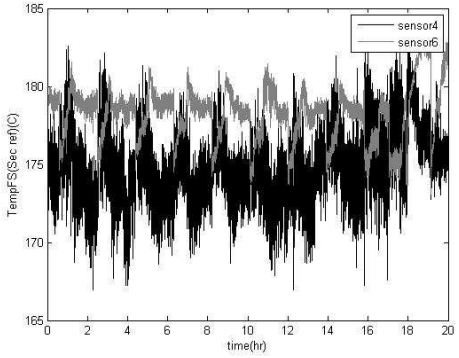

Fig. 32: Close up of the temperature responses in two positions (Sensor 4; 95 mm and sensor 6; 150 mm from the inner part of the periphery segment) for the secondary refiner.

The same situation as described for Twin refiners occurs also in CD-refiners but the settling time is shorter, see *Fig. 33*. The motor load represents the total work distributed in the flat zone and the CD-zone and the overshoot is about 3 MW during 15 minutes. It is easy to estimate the economic impact for that start-up procedure if knowing the number of start-ups.

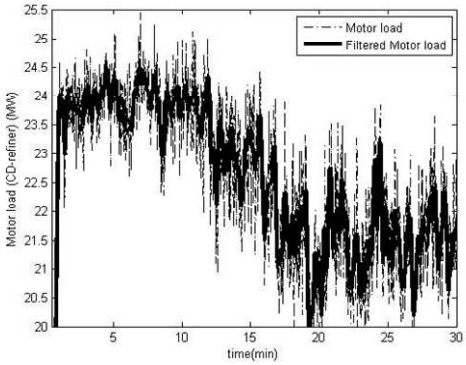

Fig. 33: Motor load during a start-up procedure in a CD-refiner (Filter constant according to Fig. 25).

According to the set of equations describing the extended entropy model above both the thermodynamical work, w_{th}, and the defibration/fibrillation work, w_{def}, are included in the total work, see further Karlström and Eriksson (2014a,b). This means that we have access to important information about the irreversible work in several positions along the radius.

As seen in *Fig. 34*, the over shoot in the defibration work is about 50% in the CD-zone compared with the overshoot in the motor load which is about 15% while the change in defibration work in the flat zone is negligible. For other positions a completely different situation may occur depending on the fiber packing degree as described above. This is important information as the defibration work clearly will affect the final pulp property. As we obviously must consider a spatial fiber distribution, which is most often overlooked in the research literature of refining theory, it is important to stress that follow up of refining processes in a dynamic perspective always should be performed if the aim is to reduce the pulp property variations and the electricity cost.

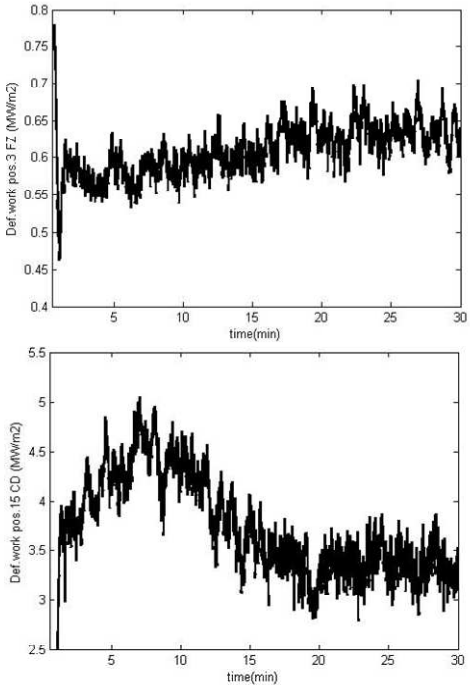

Fig. 34: Defibration work in two positions; pos. 3 close to the contraction zone in the flat zone and pos. 15 close to the periphery of the refining segment in the CD-zone.

Even though the examples could be seen as a negligible saving it is well known that “small streams make great rivers” and solving the overshoot problem in the examples outlined in *Fig. 31* gives a saving which easily can be used to invest in a new refiner control system. However, to cope with the economic considerations given above good models should be used and that will be shown later in this series of papers.